TANDEM

Research and Innovation Action (RIA)

Funded by the European Union. Views and opinions expressed are however those of the author(s) only and do not necessarily reflect those of the European Union or he European Atomic Energy Community ('EC-Euratom'). Neither the European Union nor the granting authority can be held responsible for them.

Start date : 2022-09-01 Duration : 36 Months

Report of operational transient safety case Studies for a SMR with cogeneration

Authors : Mr. Sebastian BUCHHOLZ (GRS), Alessandro De Angelis

TANDEM - Contract Number: 101059479

Project officer: Angelgiorgio IORIZZO

Document title	Report of operational transient safety case Studies for a SMR with cogeneration
Author(s)	Mr. Sebastian BUCHHOLZ, Alessandro De Angelis
Number of pages	30
Document type	Deliverable
Work Package	WP4
Document number	D4.3
Issued by	GRS
Date of completion	2025-04-01 07:58:54
Dissemination level	Public

Summary

Report of operational transient safety case Studies for a SMR with cogeneration. The safety cases to simulate will be distributed between all the participants. The safety cases studies will be performed using the (coupled) simulation models developed in WP2. For all cases, stand-alone calculations with ATHLET and CATHARE will be performed as a baseline.

Approval

Date	By
2025-04-02 12:08:49	Mrs. Natalia RODIONOV (IRSN)
2025-04-02 12:46:04	Dr. Claire VAGLIO-GAUDARD (CEA)

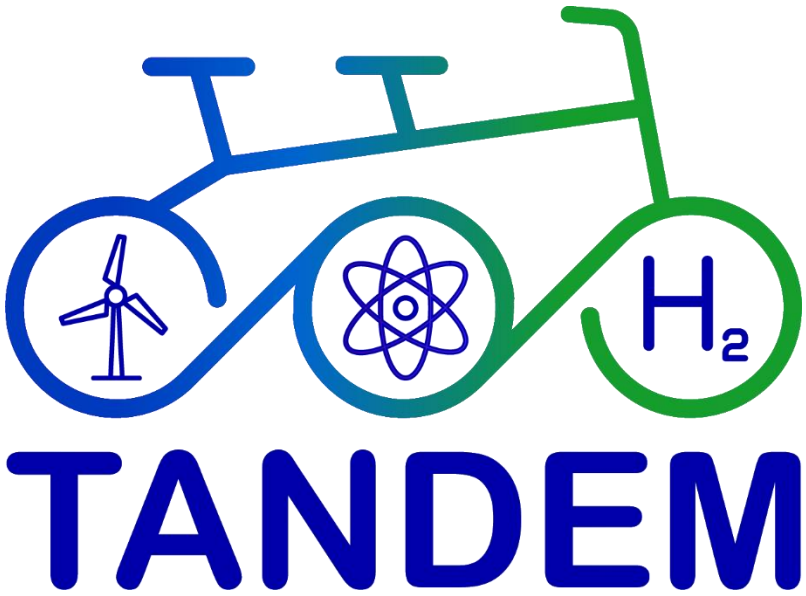

D4.3 – Report of operational transient safety case studies for a SMR with cogeneration

WP4 - Task 4.3

March 31st, 2025 [M31]

Sebastian Buchholz (GRS)

Alessandro De Angelis (UNIPI)

Funded by the European Union

Funded by the European Union. Views and opinions expressed are however those of the author(s) only and do not necessarily reflect those of the European Union or the European Atomic Energy Community ('EC-Euratom'). Neither the European Union nor the granting authority can be held responsible for them.

History

Date	Version	Submitted by	Reviewed by	Comments
31/03/2025	1	Sebastian Buchholz Alessandro De Angelis	Andreas Wielenberg (GRS)	

Funded by the European Union

Funded by the European Union. Views and opinions expressed are however those of the author(s) only and do not necessarily reflect those of the European Union or the European Atomic Energy Community ('EC-Euratom'). Neither the European Union nor the granting authority can be held responsible for them.

Table of Contents

Funded by the European Union

Funded by the European Union. Views and opinions expressed are however those of the author(s) only and do not necessarily reflect those of the European Union or the European Atomic Energy Community ('EC-Euratom'). Neither the European Union nor the granting authority can be held responsible for them.

List of Figures

Funded by the European Union

Funded by the European Union. Views and opinions expressed are however those of the author(s) only and do not necessarily reflect those of the European Union or the European Atomic Energy Community ('EC-Euratom'). Neither the European Union nor the granting authority can be held responsible for them.

Abbreviations and Acronyms

Acronym	Description
AOO	Anticipated Operational Occurrences
CSA	Cross Section Area
CSG	Compact Steam Generator
DBA	Design Basis Accident
DEC-B	Design Extension Condition with core degradation
GCSM	General Control Simulation Module within ATHLET
NSSS	Nuclear Steam Supply System
SMR	Small Modular Reactor
PI	Proportional-Integral
PID	Proportional-Integral-Derivative
PWR	Pressurized Water Reactor
TDV	Time-Dependent Volume
WP	Work Package

Funded by the European Union

Funded by the European Union. Views and opinions expressed are however those of the author(s) only and do not necessarily reflect those of the European Union or the European Atomic Energy Community ('EC-Euratom'). Neither the European Union nor the granting authority can be held responsible for them.

Executive Summary

The European TANDEM project addresses SMR safety issues related to the SMR integration into a hybrid energy system. Using a coupling between thermal-hydraulic system codes with MODELICA this integration is simulated in the frame of TANDEM. As a basis for the related SMR design, the E-SMR [1] was chosen as use-case in TANDEM. While the development of the coupling between CATHARE and MODELICA as well as the CATHARE input deck is reported in D2.6 [2], the similar work done for ATHLET is given in D2.7 [3].

This report deals with the AOOs investigated in TANDEM. The work was distributed between the project partners GRS and UNIPI. UNIPI used a quasi-static BOP model. That means, that the output variables of the BOP model are instantaneously affected by the imposed boundary conditions. In contrast, GRS used a dynamic BOP model in which the component dynamics in the BOP model are considered.

GRS performed simulations regarding the sudden increase and decrease of energy demand of the heat users. Reference initial conditions are a SMR at full power, in which the generated steam is distributed to provide 25 MW_{th} process heat for cogeneration purposes; the rest of the steam is used for electricity generation. Under these conditions, a sudden drop and increase of heat demand was simulated using the modelling devices of a cogeneration valve and an oil mass flow rate to adjust heat take-up. Additionally, the initial condition was changed to 46 MW_{th} cogeneration heat load, which corresponds to a 100 % open cogeneration valve with subsequent drop of the heat demand by closing the valve to 10 %.

The GRS simulations show that the selected nuclear facility including the balance-of-plant (BOP), and nuclear steam supply system control (NSSS control) models are basically able to cope with all proposed AOOs. However, in case of a sudden increase of thermal demand it might be necessary to additionally limit core power using provisions for operational power control. Otherwise, core power could exceed its maximum threshold allowed by the reactor protection system, which depends on the plant design.

The simulations of UNIPI also consider a thermal load rejection of the cogeneration part. Here, the core power was controlled just by the neutronic feedbacks since the low temperature deviations of the primary coolant did not trigger the operation of the control rods. It can be seen that the E-SMR settles at a slightly higher power after the load rejection than it had before. However, it was shown that the CATHARE 3 – MODELICA coupling is sufficiently stable to cope with the steep changes in boundary conditions that make it applicable for safety demonstration purposes as well.

Funded by the European Union

Funded by the European Union. Views and opinions expressed are however those of the author(s) only and do not necessarily reflect those of the European Union or the European Atomic Energy Community ('EC-Euratom'). Neither the European Union nor the granting authority can be held responsible for them.

Keywords

SMRs, Hybrid energy Systems, Safety Methodology, Flexibility, Cogeneration, Europe, AC²/ATHLET, CATHARE

Funded by the European Union

Funded by the European Union. Views and opinions expressed are however those of the author(s) only and do not necessarily reflect those of the European Union or the European Atomic Energy Community ('EC-Euratom'). Neither the European Union nor the granting authority can be held responsible for them.

1. Introduction

Within the IAEA Nuclear Energy Series No. NP-T-1.17 Guidance on Nuclear Energy Cogeneration [4], two issues from the safety point of view are mentioned: The first one is related to potential ingress of radioactive material from the nuclear plant into the cogeneration facility. The second one refers to “reactor system transients induced by the cogeneration plant”. One point to consider for the latter are sudden changes in heat or electricity demand, which could cause disturbances on the secondary side of the proposed PWR-like SMR. These disturbances could lead to fault conditions in the reactor system, which would have to be considered as postulated initiating events in safety analysis (see IAEA SSG-2 (Rev. 1) [9]) and classified as anticipated operational occurrences (AOO) or even design basis accidents (DBA). Such fault conditions would particularly arise due to unacceptable values of decoupling criteria for the cogeneration plant and the reactor system in the safety demonstration. It therefore has to be shown that the plant response to most sudden changes in heat or electricity load is suitably controlled by the provisions for operational power control in order to prevent progression to a potential DBA. Thus, the safety class 1 (and 2) provisions can reliably prevent any progress towards DEC and in particular DEC-B for all such events.

The European TANDEM project addresses SMR safety issues related to SMR integration into a hybrid energy system. Within the frame of TANDEM, feasibility studies of the hybrid system were performed. The safety scenarios that were studied ranged from normal operation to AOOs and DBAs. Generally, normal operation and AOOs are particularly impacted by the cogenerating setup of the power plant and/or by the interaction between the plant and the hybrid energy system.

To perform safety analysis of such hybrid systems using best estimate approaches, the coupling of thermal-hydraulic system codes for the reactor system with MODELICA, used to represent the non-nuclear part of the hybrid facility, was part of the TANDEM project. Due to the coupling, feedback from the MODELICA model to the system code model and vice versa can be considered in simulations. A hybrid system consisting of the E-SMR thermal-hydraulic system code model and a cogeneration model in MODELICA was used to simulate the sudden increase or decrease in thermal load due to fast electricity or heat demand changes.

The work was distributed among the partners. GRS simulated the sudden increase and decrease of thermal load from the heat users, while UNIPI investigated the case of sudden drop in electricity demand. ATHLET and CATHARE were used by GRS and UNIPI, respectively to model the E-SMR. First, the coupled models used are briefly described with respect to changes to the already documented models of the plant and the cogeneration setup in the related TANDEM deliverables. Then, the simulation results of the different cases are presented and discussed, and potential lessons learned are documented.

Funded by the European Union

Funded by the European Union. Views and opinions expressed are however those of the author(s) only and do not necessarily reflect those of the European Union or the European Atomic Energy Community ('EC-Euratom'). Neither the European Union nor the granting authority can be held responsible for them.

2. ATHLET/MODELICA simulations

2.1 Overview about ATHLET model of the E-SMR

Some modifications of the ATHLET model have been made with respect to the deliverable D2.7 [3]. In this report, the coupling of ATHLET and MODELICA is presented including first simulations verifying its applicability using two MODELICA sub models, the NSSS control and the BOP model. The BOP model, considering the system dynamics, was developed with the ThermoPower MODELICA library. The adopted BOP model is described in the project deliverable D2.3 [5].

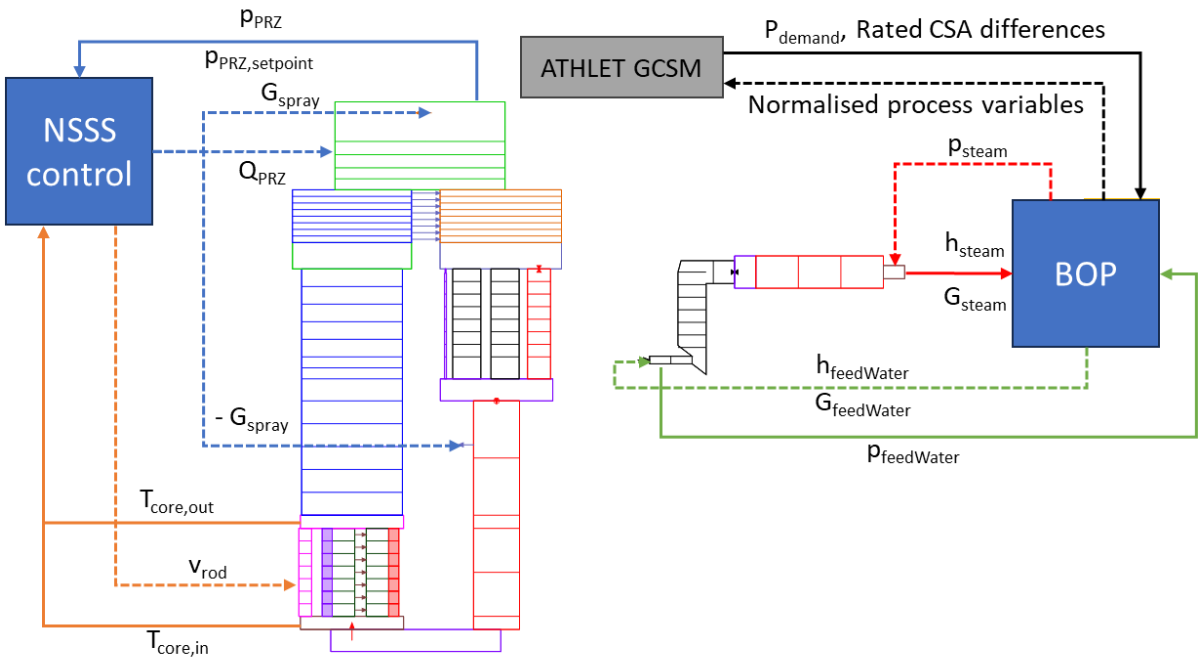

Figure 1: Coupling interfaces used for coupled simulations: dashed lines: MODELICA → ATHLET, solid lines: ATHLET → MODELICA

The coupled model is shown schematically in Figure 1 including the exchanged variables between ATHLET and the two MODELICA models used (the submodels of the NSSS control and the BOP). Although ATHLET GCSM is stated in the figure only for demanded power, rated cross section area (CSA) differences and the normalised process variables (i.e. the error signals mentioned in Table 1), GCSM is used for all of the data exchange between the two MODELICA models and ATHLET. However, the coloured arrows show the exchanged parameters given by/to time-dependent volumes and fills. The core outlet and inlet temperatures as well as the control rod velocity are exchanged between the NSSS model and ATHLET. The spray mass flow rate is added to the pressurizer by a fill and drained from the downcomer below the main coolant pump (indicated by a negative sign in the figure).

Funded by the European Union

Funded by the European Union. Views and opinions expressed are however those of the author(s) only and do not necessarily reflect those of the European Union or the European Atomic Energy Community ('EC-Euratom'). Neither the European Union nor the granting authority can be held responsible for them.

Some additional inputs were added to the ATHLET thermal-hydraulic model with respect to D2.7 [3] since the control of various valves in the MODELICA part was given to ATHLET. These valves are shown in the scheme of the model in Figure 2 and controlled by means of ATHLET GCSM using PI controllers. A description of the usage of the valves is given in Table 1.

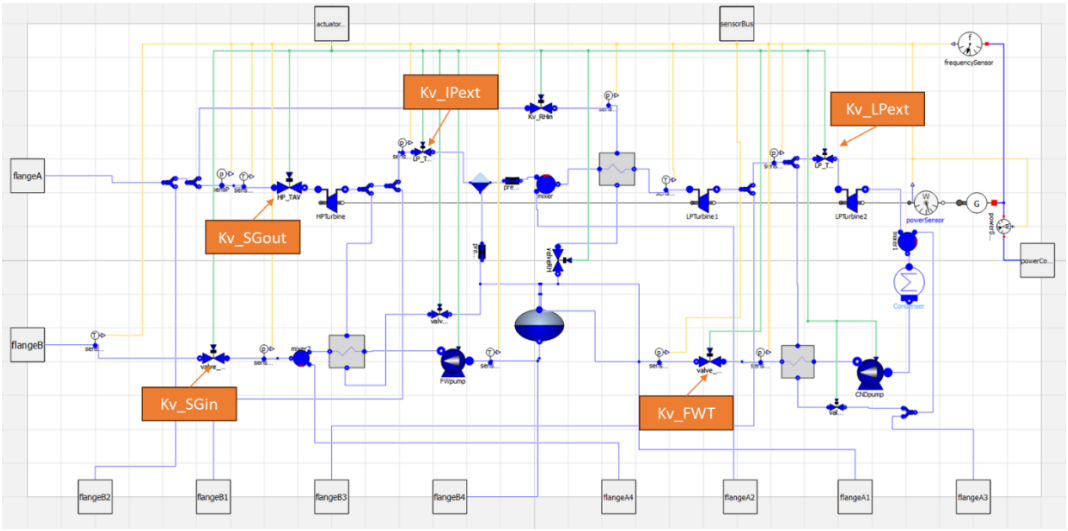

Figure 2: BOP model developed with ThermoPower [5]

Table 1: Description of valves of BOP controlled externally

Valve name	Description	Corresponding process variable
SGout	High pressure turbine admission valve	Turbine rotation speed
SGin	Steam generator admission valve	Main steam pressure
IPext	Intermediate pressure control valve	Intermediate pressure
LPext	Low pressure control valve	Low pressure
FWT	Feed water tank admission valve	Feed water tank pressure
bypass	Bypass valve	Manually moved
CoGeneration	Cogeneration valve	Manually moved

The CSAs of the valves can be changed by ATHLET. The control on how to change valve CSA is based on a relative difference of a specific process variable and from its setpoint. This rated error signal is an output of the BOP model and can be used in ATHLET to control the valve CSA. Either a PIDT1 controller or an explicitly modelled PI controller (using GCSM integrator and adder controller) have been used to perform this control. The advantages of the separate treatment are the upper and lower limits of the integrator controller, which are not provided by the PIDT1 controller [10]. In some cases, in which the integrator part in the PIDT1 controller is already large, the respective valve response might be too late, e.g., if the controller input (i.e. the error signal) changes sign.

The output of ATHLET given to MODELICA is a rated value of the CSA in the range of [-0.99, 0] in which 0 is fully open and -0.99 is closed. The exceptions are the turbine bypass and

Funded by the European Union

Funded by the European Union. Views and opinions expressed are however those of the author(s) only and do not necessarily reflect those of the European Union or the European Atomic Energy Community ('EC-Euratom'). Neither the European Union nor the granting authority can be held responsible for them.

the cogeneration valves, for which the range is [0, 0.99] with 0 fully closed and 0.99 fully opened. Both valves are not controlled by a dedicated PIDT1 controller in ATHLET but are set explicitly by means of time function. The turbine bypass valve could be used for damping the pressure increase when the load to the turbine or cogeneration heat demand is rejected. The cogeneration valve is used to control the amount of heat for cogeneration purposes. Cogeneration is simulated in the BOP model by heating up an oil flow. The oil mass flow rate is controlled by the cogeneration valve rated CSA in ATHLET as well and given to the MODELICA model.

Another parameter set in ATHLET and given to the BOP model is the demanded electrical power. Changing this parameter directly influences the torque of the turbine which leads to an increase or drop of its rotation speed. Compensation is done by the aforementioned high pressure turbine admission valve, which is closed if the rotation speed decreases which leads to a decreasing difference of the actual value and the setpoint (negative error), and opened if the speed increases.

2.2 Investigated AOOs

During the project it was agreed to investigate the sudden increase and decrease of the energy demand of the heat users by using ATHLET and the MODELICA models. Given that such a fault could likely happen during the lifetime of the plant, the sudden drop or increase of demanded heat power is classified as an anticipated operational occurrence (AOO), based on the stated criteria, e.g., in IAEA SSG-2 (Rev. 1) [9].

Two different cases are simulated concerning the decrease of power demand by the heat users. First, the sudden drop of heat demand from 50 % to 3 % in 10 s is considered. In the second case, the drop is even larger - from 100 % to 10 % (also in 10 s). The cases are listed in Table 2 (No. 1 and 2). The drop is simulated by closing the cogeneration valve to 3 % or 10 % respectively including a reduction of the oil mass flow rate to the same values.

Table 2: Investigated power demand from the heat users - cases

No.	Case	Notes
1	Full core power distributed to 25 MW_{th} cogeneration, rest (164.8 MW_{el}) electrical power	Drop from 50 % to 3 % in 10 s
2	Full core power distributed to 46 MW_{th} cogeneration, rest (153.0 MW_{el}) electrical power	Drop from 100 % to 10 % in 10 s
3	Full core power distributed to 25 MW_{th} cogeneration, rest (164.8 MW_{el}) electrical power	Increase from 50 % to 100 % in 10 s

The third case is the sudden increase in thermal load by opening the cogeneration valve to 100 % in 10 s. This case is listed in Table 2 with No. 3.

Funded by the European Union

Funded by the European Union. Views and opinions expressed are however those of the author(s) only and do not necessarily reflect those of the European Union or the European Atomic Energy Community ('EC-Euratom'). Neither the European Union nor the granting authority can be held responsible for them.

2.3 ATHLET/MODELICA simulation results

In all cases, the initial conditions cover a full power E-SMR (540 MW_{th}). The secondary steam mass flow rate is distributed in case 1 and 3 to provide 25 MW_{th} cogeneration heat and 164.8 MW_{el} electrical power. In case 2, the cogeneration valve is opened to 100 % leading to a cogeneration power of approximately 46 MW_{th}. The rest is used to generate electrical power of 153 MW_{el}. In the simulation, at t = 0, the cogeneration valve is either closed to a certain value or fully opened in 10 s.

2.3.1 Case 1 and 2: Sudden decrease of heat demand

The simulation results on the drop of the cogeneration heat demand from 50 % to 3 % is shown in Figure 3. At 0 s, the cogeneration valve and oil mass flow rate are decreased to 3 % in 10 s. The drop is shown in Figure 3 top left. As a response, the main steam pressure increases (Figure 3 top right) leading to a decrease of steam generator power (Figure 3 bottom left). The difference between core power and steam generator power corresponds to the power of about 2.5 MW provided by the main coolant pumps inside the primary system.

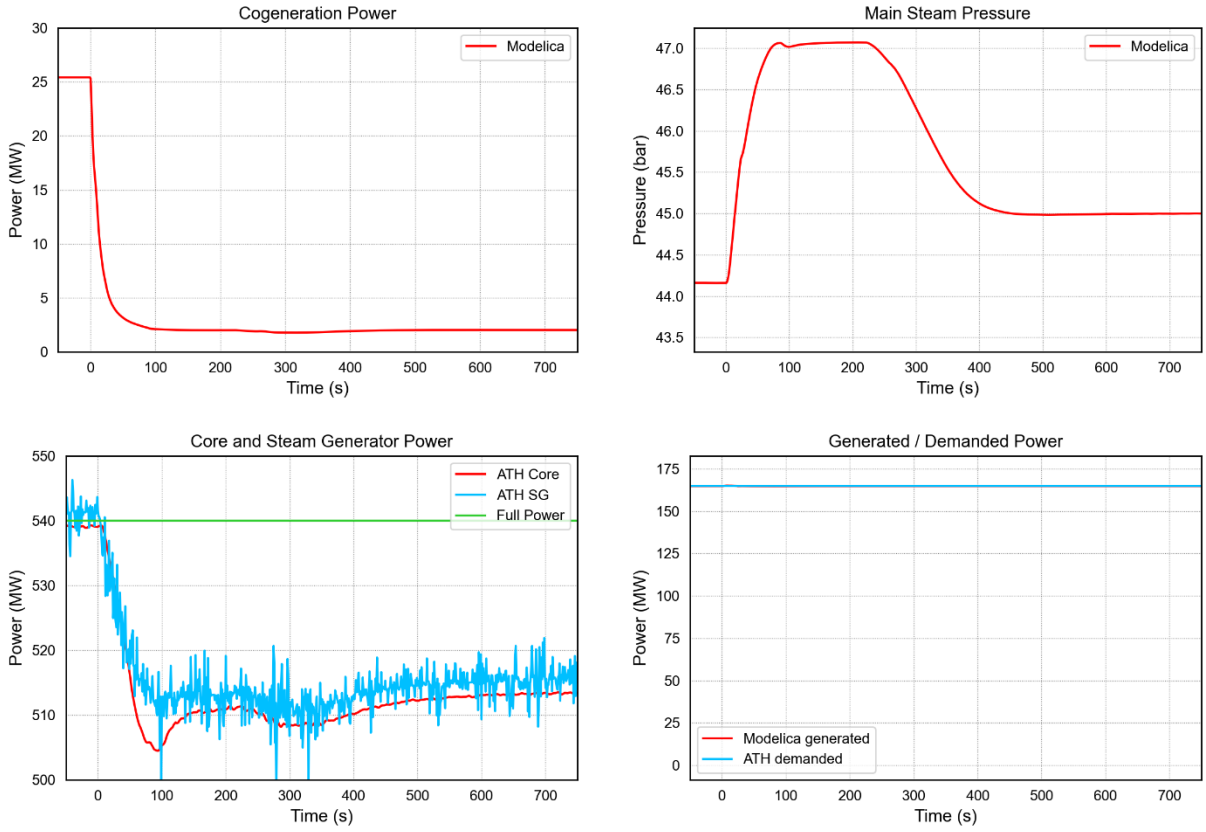

Figure 3: Behaviour of the coupled system during case 1, power and pressure evolutions

The electrical power supply is constant over time (Figure 3 bottom right). Due to lower steam generator power, the primary temperature is increasing as indicated by the average coolant

Funded by the European Union

Funded by the European Union. Views and opinions expressed are however those of the author(s) only and do not necessarily reflect those of the European Union or the European Atomic Energy Community ('EC-Euratom'). Neither the European Union nor the granting authority can be held responsible for them.

temperature (Figure 4 top left). The density of the coolant decreases leading to a negative reactivity feedback due to less moderation (see Figure 4 top right). The power decreases leading to lower fuel temperature, which in turn leads to a positive Doppler feedback. This feedback is compensated by the control rod external reactivity. The control rods are moved due to the coolant temperature control, which drives the rods into the core when the average fluid temperature in the core increases. Primary pressure increases slightly (Figure 4 bottom left), which is damped by the spray system that keeps the primary pressure almost constant. The safety valves are not triggered since the primary and secondary pressures are kept below their set limits (which are 172.3 bar and 84.5 bar for the primary and secondary safety valves). In the simulation, the AOO is controlled by systems that usually control AOOs and maintain normal operation.

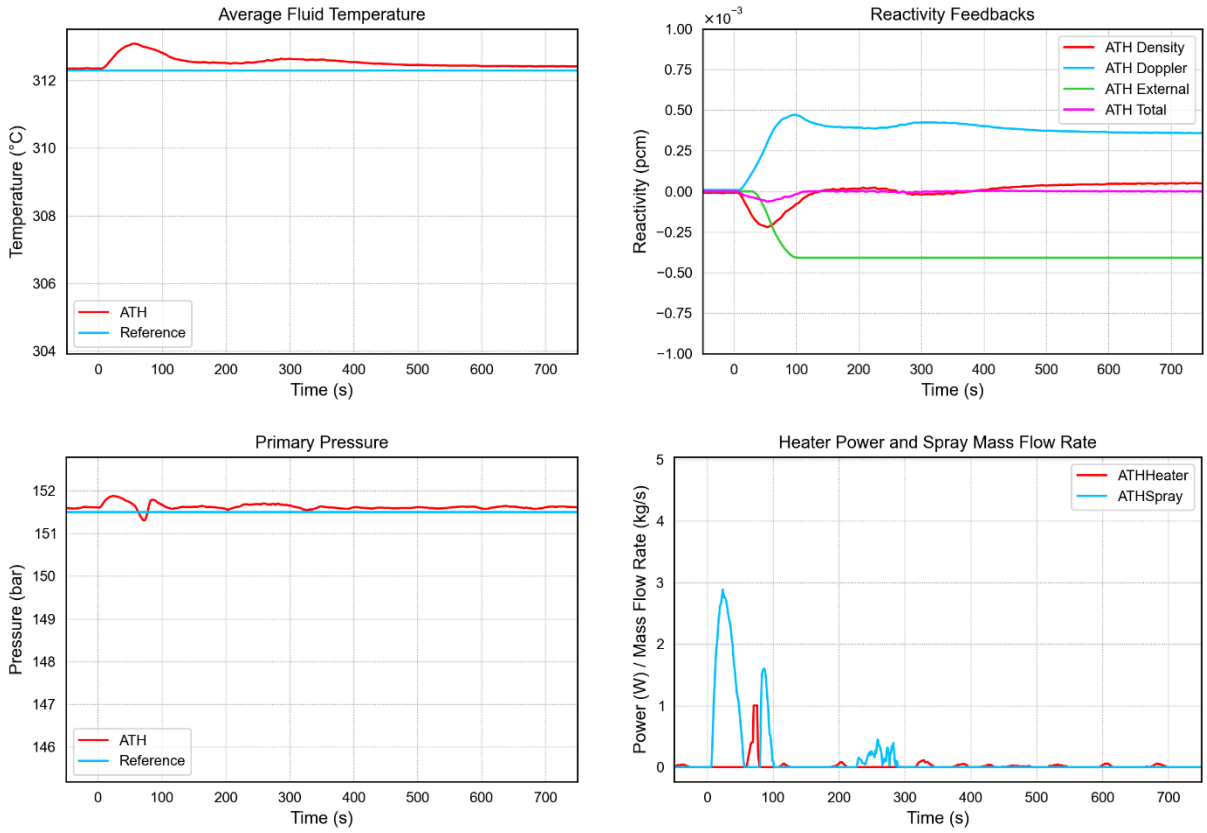

Figure 4: Behaviour of the coupled system during case 1, power and pressure control including reactivity feedback

The behaviour of the ATHLET GCSM controlled MODELICA valves is shown in Figure 5. The errors on the left side are approximately zero during the initial phase, except for the steam generator input pressure (Psg) that shows a small offset. The related valve would need to be opened further, but it is already fully opened. The relative CSAs (shown on the right) are constant during the initial steady state. With closing the cogeneration valve, the pressure of the steam generator inlet increases as indicated by the error signal (bright blue line in Figure 5 left), which is given by

Funded by the European Union

Funded by the European Union. Views and opinions expressed are however those of the author(s) only and do not necessarily reflect those of the European Union or the European Atomic Energy Community ('EC-Euratom'). Neither the European Union nor the granting authority can be held responsible for them.

MODELICA to ATHLET to control the MODELICA steam generator admission valve. Unfortunately, the response is late compared to the response of the other valves since the integrator part of the related PIDT1 controller already became large. The large negative value needs to be compensated over time by the integrator before the response can be expected, showing the drawback of using the PIDT1 controller of GCSM instead of a separated integrator/proportional contribution. However, at the end of the simulation, all valves are kept constant in their position with very small control offsets.

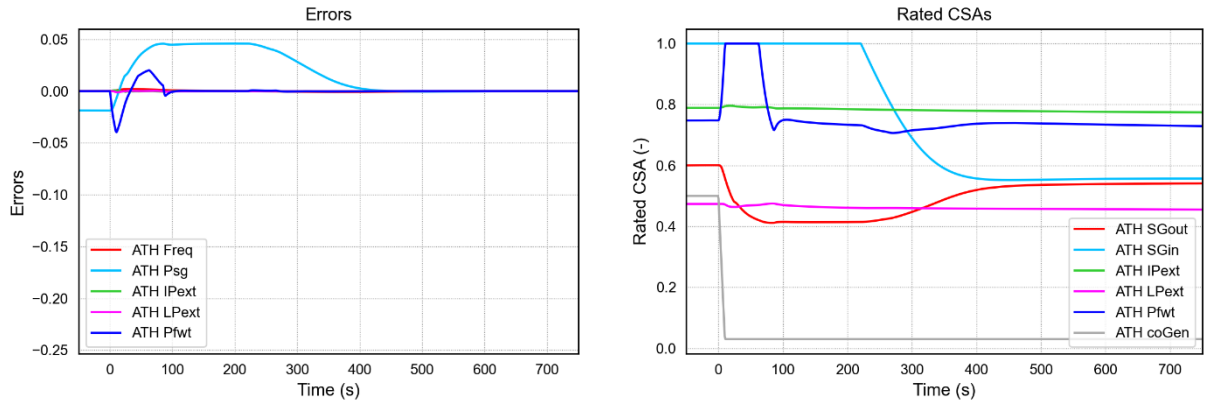

Figure 5: Behaviour of the coupled system during case 1, valve control

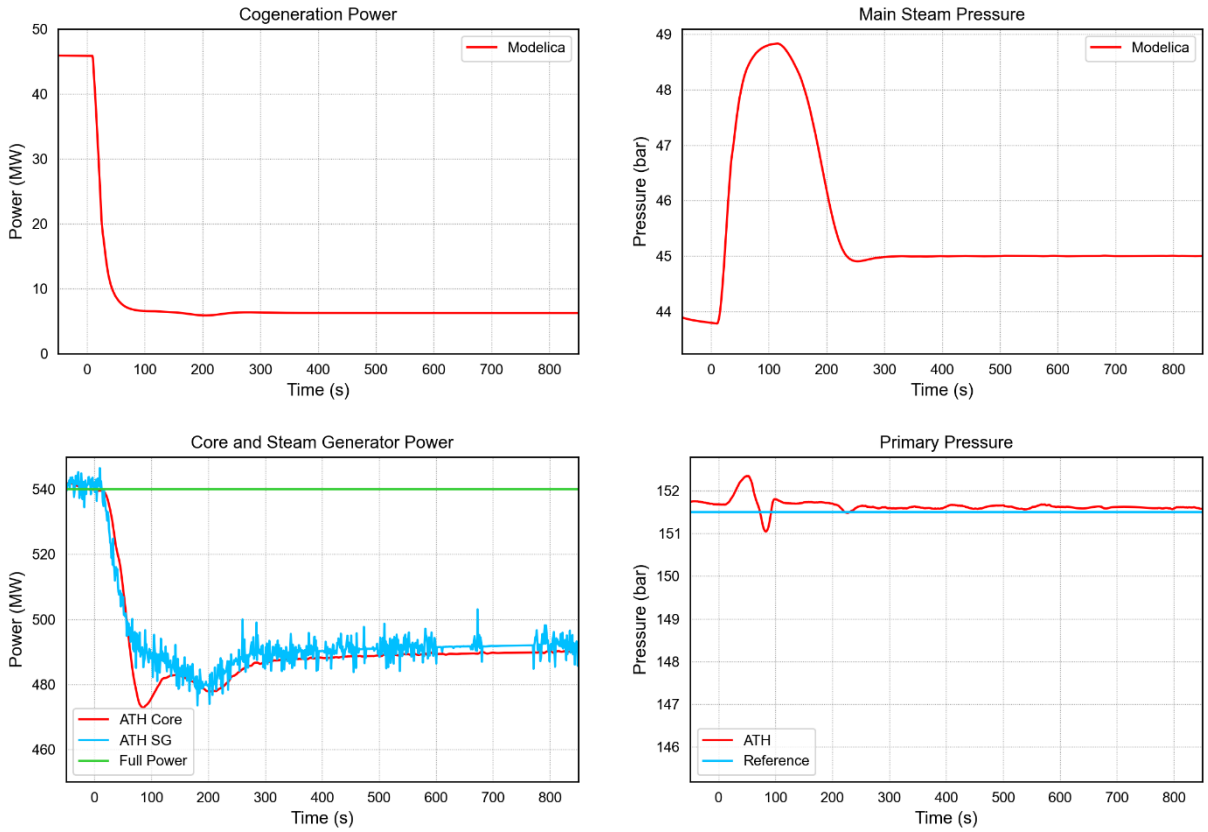

Figure 6: Behaviour of the coupled system during case 2

Funded by the European Union

Funded by the European Union. Views and opinions expressed are however those of the author(s) only and do not necessarily reflect those of the European Union or the European Atomic Energy Community ('EC-Euratom'). Neither the European Union nor the granting authority can be held responsible for them.

Case 2 (Figure 6), in which the heat demand decreases rapidly from 100 % to 10 %, does not differ much from the previous case. The main difference is the larger power drop, which consequently can be seen in the power drop of the E-SMR core. The phenomena related to this AOO remain the same. The secondary pressure increases to a little less than 49 bar, which is still lower than the set point of the pressure limitation. The same response applies for the primary pressure.

In conclusion, in both cases 1 and 2, it can be noted that the simulated E-SMR coupled with the BOP system is able to resist the proposed AOOs with BOP systems only (not using safety class 1 or 2 systems) and without extending the AOO to a DBA. To proof whether a stronger ramp led to the same conclusions, further simulations would be needed.

2.3.2 Case 3: Sudden increase of heat demand

For this case, the initial conditions are the same as in case 1. However, when a sudden increase in heat demand occurs at full core power, the main steam pressure decreases leading to an increasing steam generator pressure, which consequently leads to increasing core power (that all can be seen in Figure 7), while the produced electrical power is kept constant.

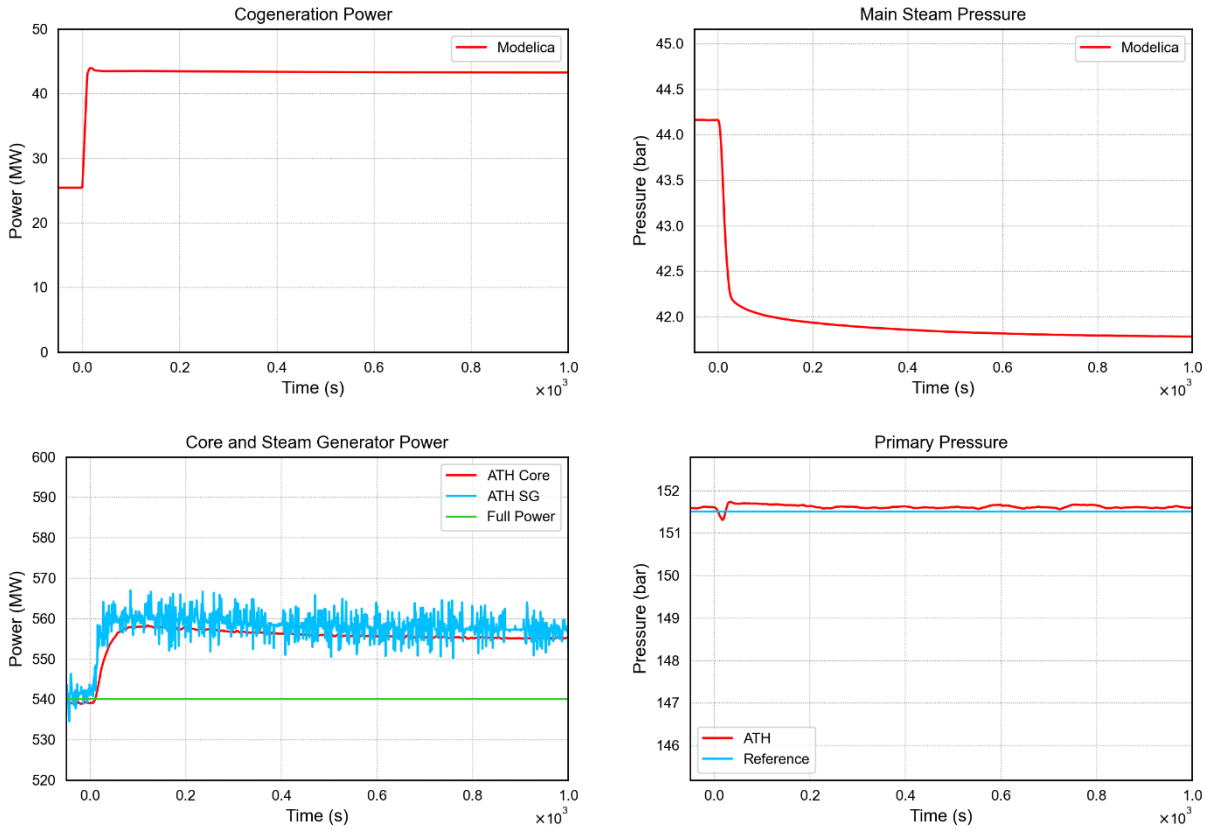

Figure 7: Behaviour of the coupled system during case 3

The lower secondary side saturation temperature consequently leads to a lower core inlet temperature. The higher core power increases the heat-up over the core. However, the core

Funded by the European Union

Funded by the European Union. Views and opinions expressed are however those of the author(s) only and do not necessarily reflect those of the European Union or the European Atomic Energy Community ('EC-Euratom'). Neither the European Union nor the granting authority can be held responsible for them.

outlet temperature in the simulation does not increase due to the decreased core inlet temperature. Also, the cladding temperature is decreasing as indicated by the maximum cladding temperature in the simulation. This behaviour is shown in Figure 8. However, due to the higher core power, the departure from nucleate boiling ratio decreases.

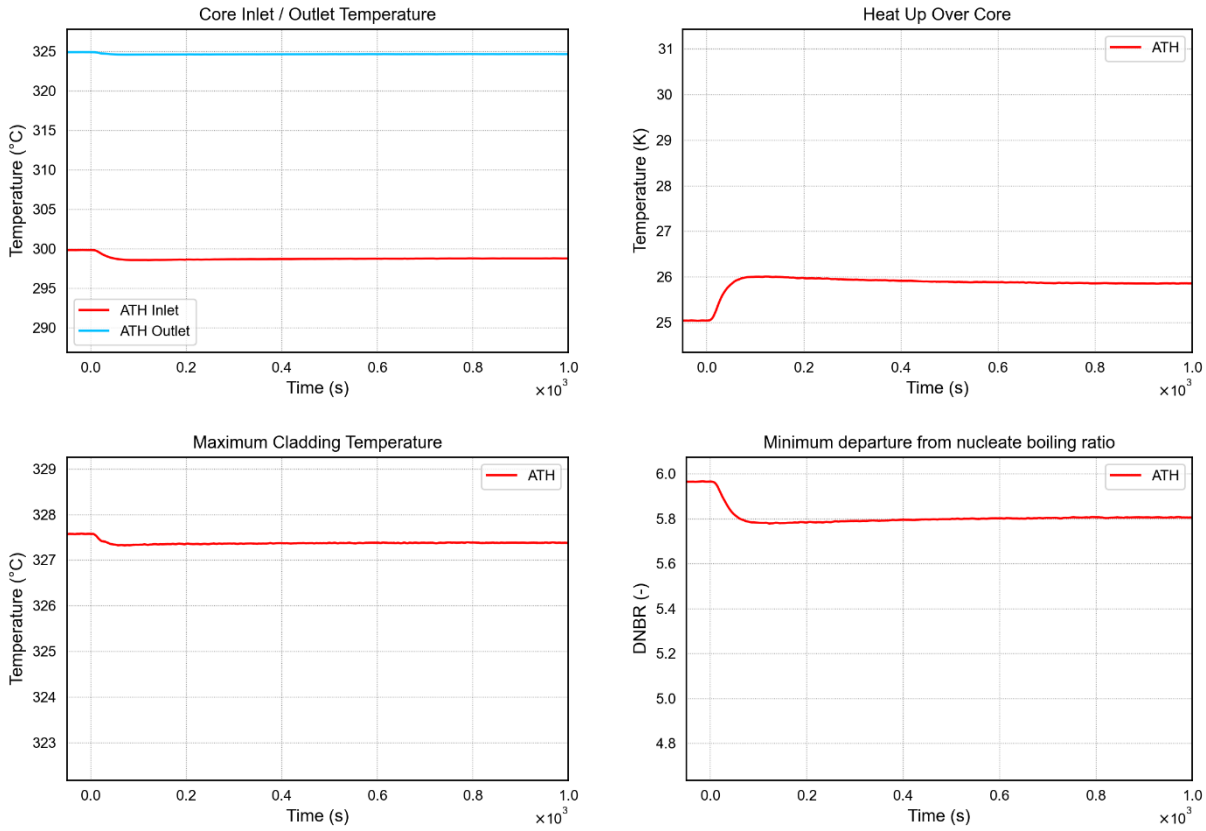

Figure 8: Behaviour of the coupled system during case 3, Core Temperature and DNBR

Although the simulation of this case does not lead to thermal-hydraulic conditions which directly cause a SCRAM, the excess of core power in the E-SMR might be beyond typical safety limits, depending on the actual design of the plant. The increase is about 3.7 % based on the nominal core power, which is lower than the shutdown criterion of approximately 106 % applied in many current large PWR plants.

3. CATHARE/MODELICA simulations

3.1 Overview about E-SMR CATHARE 3 Model Implementations

The general layout of the CATHARE 3 model of the E-SMR was not modified with respect to the one illustrated in the deliverable D2.6 [2], hence it is not described in this document. However, a few implementations were introduced regarding the reactivity control systems, which are briefly

Funded by the European Union

Funded by the European Union. Views and opinions expressed are however those of the author(s) only and do not necessarily reflect those of the European Union or the European Atomic Energy Community ('EC-Euratom'). Neither the European Union nor the granting authority can be held responsible for them.

explained below for better understanding the results of the analyses described in the next sections.

The reference core neutronic parameters introduced in the CATHARE 3 E-SMR model, i.e. decay constants and delayed neutron fractions of each precursor, are those implemented in the MODELICA model of the Nuclear Steam Supply System (NSSS) by the partners involved in its modelling [5]. The reactivity feedback coefficients of moderator and Doppler effect, instead, were kept unchanged with respect to those already implemented in the E-SMR model. Regarding the control rods, they were modelled as an external reactivity source ρ_{ext}, thus neglecting their insertion/extraction velocity and their spatial distribution. The assumption of considering the control rods as external source of reactivity was dictated by the inherent structure of CATHARE 3, which is based on a lumped parameter model to address the core kinetics (point kinetics model). The PI control function implemented in the CATHARE 3 model to command the control rods is the one expressed in eq. (1), which aims at controlling the average core coolant temperature.

$$\rho_{ext} = K_P e(t) + K_I \int_{\tilde{t}}^{t} e(t)dt \tag{1}$$

The gains of the control function, i.e. K_P and K_I, were provided by POLIMI as the reference values introduced in the MODELICA NSSS model [5]. The error function $e(t)$ was simply considered as the deviation of the average core coolant temperature T_{avg} with respect to its setpoint value T_{sp} as defined in eq. (2).

$$e(t) = T_{avg}(t) - T_{sp} \tag{2}$$

Finally, it is important to mention that a deadband of ± 0.5 °C was imposed for the control rods operation, i.e. they start to introduce reactivity in the core only if $|e(t)| > 0.5$ °C.

3.2 Thermal load rejection assessed with the quasi-static BOP model

Using the developed coupling procedure between CATHARE 3 and MODELICA, a thermal load rejection scenario was assessed using the BOP model developed with the ThermoSysPro MODELICA library [6]. The adopted BOP model is described in detail in the project deliverable D2.3 [5]. However, some of its features are also highlighted in this section to provide a better understanding of the transient setup and the results presented in the next chapter:

- The reference model of BOP is quasi-static, i.e. the component dynamics is not considered. Therefore, the model relies on lumped parameter equations to describe the component time behaviour. Consequently, any change in a boundary condition would instantaneously affect the output variables.

Funded by the European Union

Funded by the European Union. Views and opinions expressed are however those of the author(s) only and do not necessarily reflect those of the European Union or the European Atomic Energy Community ('EC-Euratom'). Neither the European Union nor the granting authority can be held responsible for them.

- The heat user, connected to the nuclear power plant for cogeneration, is represented as a thermal power boundary condition as shown in Figure 9. The cogeneration heat exchanger, modelled as an ideal condenser [5], is supplied by steam bypassed from the BOP at the outlet of the high-pressure steam turbine. The steam bypass is controlled through a control valve, also shown in Figure 9, which is regulated by a PI controller. This controller measures the heat power exchanged by the ideal condenser and compares it to the thermal power set as boundary condition, consequently controlling the bypass valve opening.

- The control systems implemented in the model rely on the quasi-static assumption. As a result, some controllers commonly found on the secondary side of a nuclear power plant, e.g. the turbine rotational speed control system, are excluded from the present BOP model. Regarding the adopted control systems [5], their parameters were maintained at default values with the exception of the main feedwater pump control system, which regulates its rotational speed based on the steam temperature exiting the Compact Steam Generator (CSG) [5]. In this regard, the proportional gain and the integration time constant of the feedwater pump controller were set to 0.1 and 3 seconds respectively. The higher integration time constant was introduced to assist the model in handling the fast variations caused by the event. Otherwise, the simulation would fail if the control parameters were left unchanged from their default values.

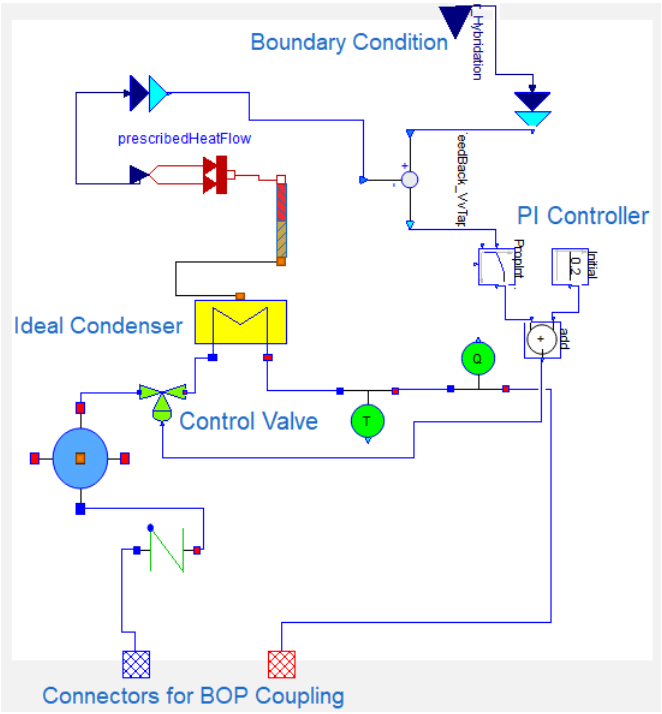

Figure 9: Cogeneration section of the ThermoSysPro BOP.

Funded by the European Union

Funded by the European Union. Views and opinions expressed are however those of the author(s) only and do not necessarily reflect those of the European Union or the European Atomic Energy Community ('EC-Euratom'). Neither the European Union nor the granting authority can be held responsible for them.

The addressed thermal load rejection event is simulated as follows:

- Starting from a stationary fully-electric power generation mode of the coupled system, the thermal power demand imposed on the cogeneration section is brought to -86.5 MW, corresponding to a heat-to-power ratio equal to 50 %, through a ramp lasting 600 s as shown in Figure 10. After 1,000 s of cogeneration, a sudden disruption of the thermal power is simulated through a ramp lasting 20 s considering e.g. a sudden failure of the heat user. In this regard, it must be mentioned that the thermal load rejection was simulated with a steep ramp and not with a step, since the adoption of a vertical drop of the thermal load would lead to an abnormal disruption of the co-simulation.

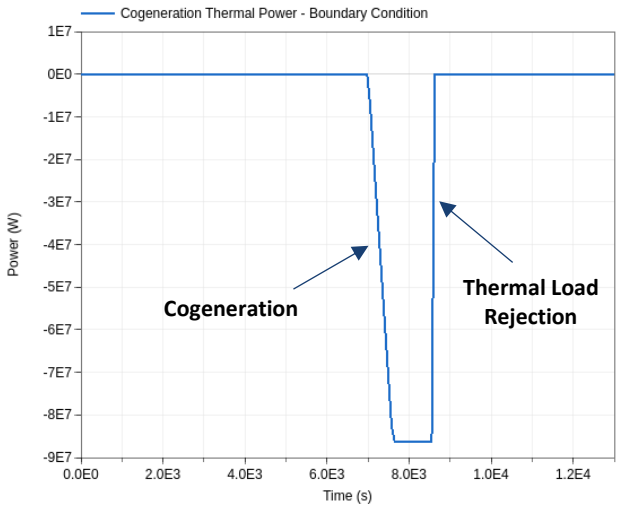

Figure 10: Adopted boundary condition for the thermal load rejection analysis.

- After the transient occurrence, the coupled system, i.e. E-SMR and BOP, is left evolving spontaneously without any external agent thanks to the implemented control systems described above and, more in detail, in the reference deliverable [4].

As shown in Figure 10, the entire analysis lasted 14,000 s of physical time. The co-simulation was supervised by Dymola 24x [7], adopting the DASSL implicit algorithm for the co-simulation supervision [8]. Figure 11 shows the coupling circuit developed with Dymola 24x.

Funded by the European Union

Funded by the European Union. Views and opinions expressed are however those of the author(s) only and do not necessarily reflect those of the European Union or the European Atomic Energy Community ('EC-Euratom'). Neither the European Union nor the granting authority can be held responsible for them.

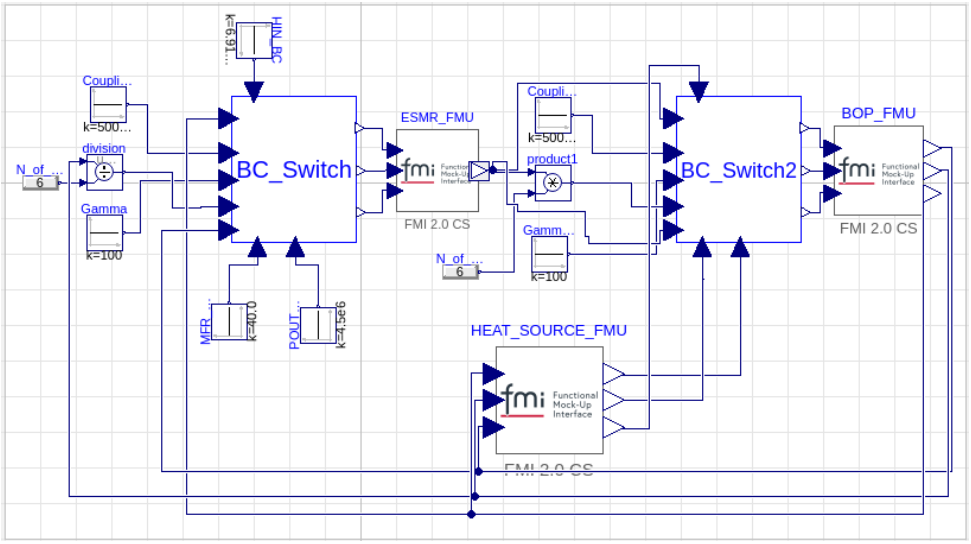

Figure 11: Coupling Circuit performed on Dymola 24x.

The seemingly long simulation time was dictated by the numerical characteristics of the CATHARE 3 code, which needs a preliminary transient simulation aiming to achieve a stationary condition (i.e., stabilized transient) before running the real transient scenario. In this regard, the entire transient analysis was divided into the following steps:

1. First, a 5,000 s stand-alone run of the two models was carried out with boundary conditions provided externally, in order to allow the models to reach stable behaviour before the coupling. In this case, the CATHARE 3 model was run with constant boundary conditions, whereas the BOP model was run coupled with a lumped parameter heat source, also belonging to the TANDEM MODELICA library [5] (see again Figure 11). The 5,000 s of the stand-alone run was comprised of 2,500 s of a stabilized transient and, after the activation of the core neutronics module, another 2,500 s of stand-alone run to assure the correct stabilization of the core neutronic parameters.

2. At 5,000 s, the coupling between the two models occurred, and the simulation was kept running in full electric mode to assure the correct stabilization of the coupled system. The switch of the boundary conditions between the stand-alone and the coupled run was performed by using specific switches developed utilizing the MODELICA Standard Library components. The developed switch models, namely *BC_SWITCH* shown in Figure 11, perform the switch between two signals y_1 and y_2 such that the output signal y is managed as in eq. (3)

$$y = \left[1 - \phi(t,\gamma)\right] y_1 + \phi(t,\gamma) y_2 \tag{3}$$

where $\phi(t,\gamma)$ is a smoothing function defined as in eq. (4)

Funded by the European Union

Funded by the European Union. Views and opinions expressed are however those of the author(s) only and do not necessarily reflect those of the European Union or the European Atomic Energy Community ('EC-Euratom'). Neither the European Union nor the granting authority can be held responsible for them.

$$\phi(t,\gamma) = \frac{1}{2}\left[1 - \tanh\left(\frac{t - t^*}{\gamma}\right)\right] \quad (4)$$

and t^* is the coupling time, i.e., 5,000 s. The present analysis was carried out using the time constant γ equal to 100 s.

3. At 7,000 s, the cogeneration transient occurred as shown in Figure 10, ending at 7,600 s.

At 8,600 s, the thermal load rejection event takes place, causing the thermal load to steeply decrease back to 0 MW. Afterwards, the system is kept evolving freely up to 14,000 s.

3.3 CATHARE/MODELICA simulation results

In this section, the results obtained by the thermal load rejection assessment with a quasi-static BOP model are presented. For purposes of clarity, in each figure the coupling start is highlighted with a vertical line, indicating the actual start of the coupled analysis. In general, it must be mentioned that the presented results may have been strongly influenced by the assumption of the quasi-static model of the BOP. In fact, the introduction of the component dynamics in the model could have shown different behaviours due to the delays naturally introduced by the component dynamics, which might have led, e.g., to smoother changes of the operational parameters.

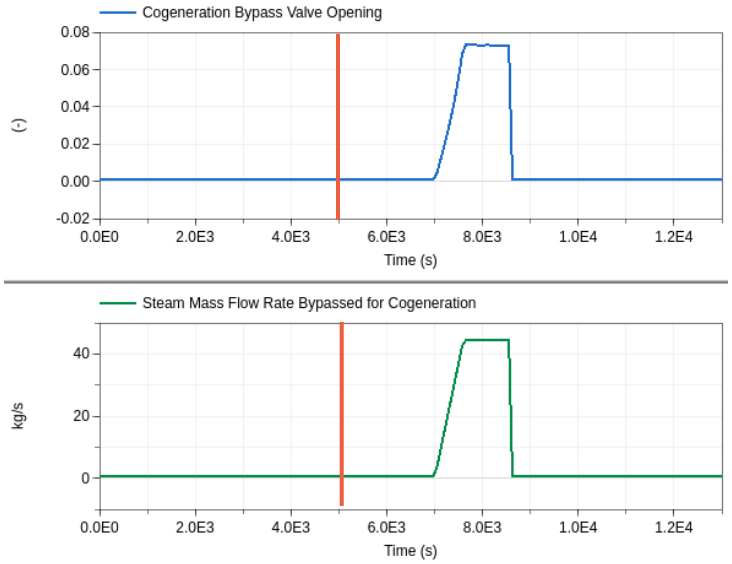

Figure 12: Cogeneration bypass valve opening and bypassed steam mass flow rate during thermal load rejection transient.

Referring to the transient description provided in Section 3.2 and to the thermal load shown in Figure 10, Figure 12 shows the cogeneration valve opening, commanded by the PI controller shown in Figure 9, and the mass flow rate of the bypassed steam from the BOP. The opening of

Funded by the European Union

Funded by the European Union. Views and opinions expressed are however those of the author(s) only and do not necessarily reflect those of the European Union or the European Atomic Energy Community ('EC-Euratom'). Neither the European Union nor the granting authority can be held responsible for them.

the cogeneration valve led to an increase in the feedwater temperature, which in turn triggered the main feedwater pump control system that increased its rotational speed as shown in Figure 13. The feedwater temperature increases due to the return of the condensate from the ideal heat exchanger shown in Figure 9, which was merged with the feedwater coming from the pre-heaters. Thus, the enthalpy of the resulting flow increases with respect to full-electric power generation operations. For the sake of clarity, it must be reminded that the rotational speed of the main feedwater pump is controlled, in this specific case, by the steam temperature [5], which tended to increase with the rise of the feedwater enthalpy. The decrease in the feedwater temperature caused by the thermal load rejection event led to a sudden increase of the feedwater mass flow rate entering the CSG as shown in Figure 14, which peak was soon recovered bringing its value to the full electric one.

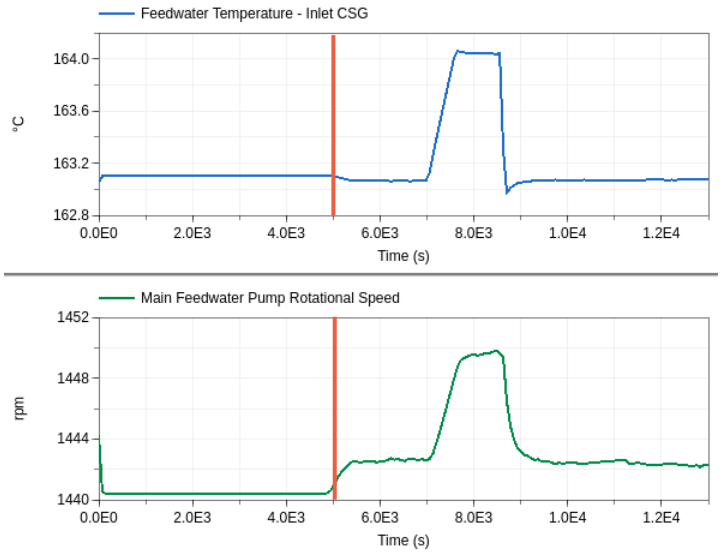

Figure 13: Feedwater temperature and main feedwater pump rotational speed achieved during the thermal load rejection transient.

In this regard, the first downward excursion of the mass flow rate depicted in Figure 14 can be attributed to the feedwater temperature rising caused by the opening of the cogeneration valve (see again Figure 13). The increase in feedwater temperature caused the temporary decrease of the mass flow rate due to the fluid expansion (i.e. density decreasing due to higher temperature) and due to the fact that the outlet pressure was kept constant by the main steam line pressure controller. Then the mass flow rate value was recovered after the end of the cogeneration transient thanks to the higher rotational speed of the pump. Afterwards, the sudden cooling down of the feedwater mass flow rate caused by the thermal load rejection sharply increased the feedwater density, hence resulting in the mass flow rate peak shown in Figure 14. Concurrently, the pump control system decreased the rotational speed of the main feedwater pump as shown in Figure 13.

Funded by the European Union

Funded by the European Union. Views and opinions expressed are however those of the author(s) only and do not necessarily reflect those of the European Union or the European Atomic Energy Community ('EC-Euratom'). Neither the European Union nor the granting authority can be held responsible for them.

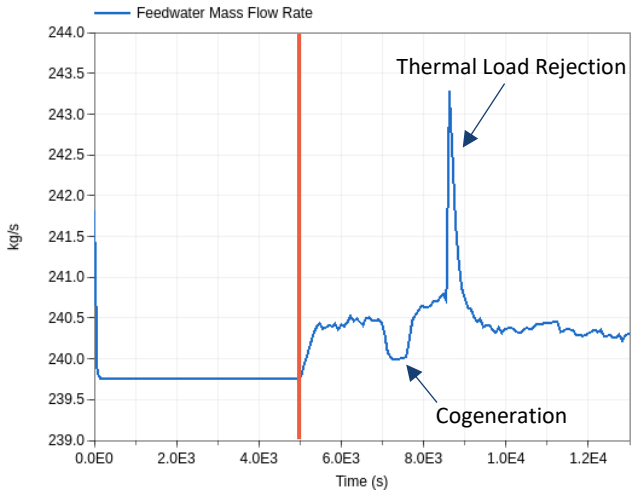

Figure 14: Feedwater mass flow rate during thermal load rejection transient.

The sudden increase in the mass flow rate caused by the thermal load rejection increased the CSG thermal power, thus triggering the core neutronic feedbacks due to the temporary decrease of the primary coolant temperature. In fact, as it can be noticed by Figure 15, the increase of the secondary mass flow rate led to the introduction of positive moderator reactivity, thus leading to a sharp core power rise. As a consequence, the fuel reacted by introducing negative reactivity (Doppler effect), which helped to limit the core power excursion. The superposition of both reactivity feedbacks resulted in the positive introduction of reactivity in the core shown in Figure 16 and, consequently, in the reactor power rising as mentioned above. As depicted in Figure 16, the core power reached a maximum value of 545.4 MW, which is 0.8 % higher than the reference value achieved in fully electric power generation conditions (i.e., 540.9 MW). Importantly, the core power variations were completely managed by the core neutronic feedbacks, hence it did not involve any control rod movements as shown in Figure 15. In fact, the missing operation of the control rods is caused by the fact that the decrease of the average core coolant temperature was kept within the deadband for the control rod operation, which was set equal to ± 0.5 °C, as shown in Figure 17, where the average core coolant temperature is depicted.

Funded by the European Union

Funded by the European Union. Views and opinions expressed are however those of the author(s) only and do not necessarily reflect those of the European Union or the European Atomic Energy Community ('EC-Euratom'). Neither the European Union nor the granting authority can be held responsible for them.

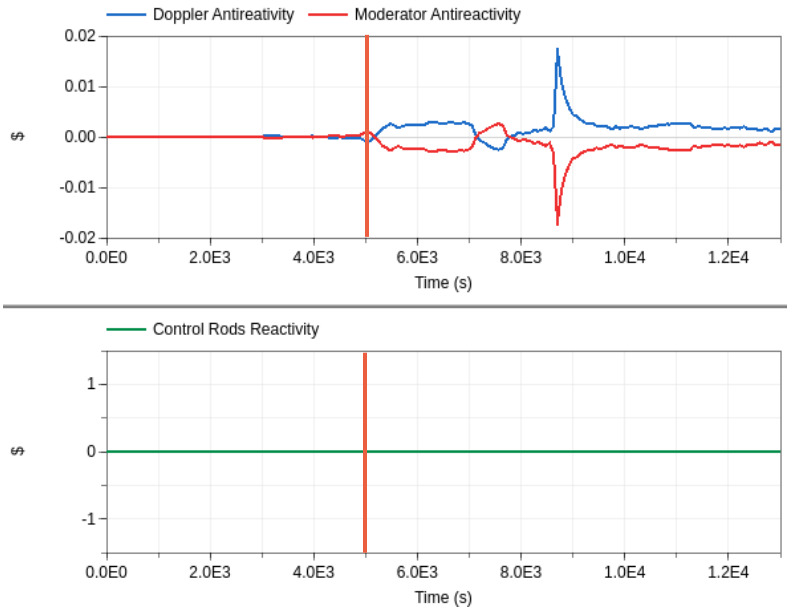

Figure 15: Reactivity feedbacks and control rod reactivity insertion during thermal load rejection transient.

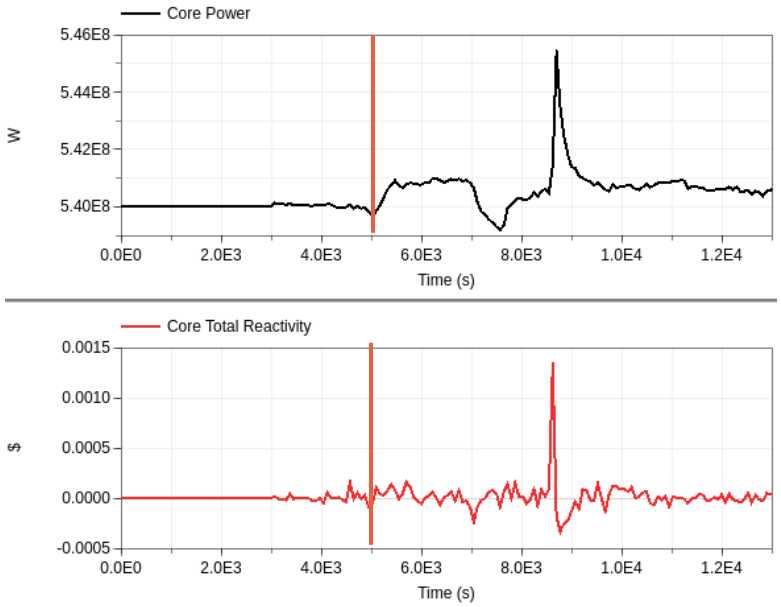

Figure 16: Core thermal power and total reactivity during thermal load rejection transient.

As a matter of fact, as it can be seen in Figure 17 and Figure 18 (where the primary pressure at core inlet is depicted), the occurrence of thermal load rejection had a mild influence on the primary coolant temperature and pressure. The predicted average core coolant temperature deviation during the considered event, indeed, was about 0.2 °C, whereas the primary pressure was found to decrease by about 1 bar.

Funded by the European Union

Funded by the European Union. Views and opinions expressed are however those of the author(s) only and do not necessarily reflect those of the European Union or the European Atomic Energy Community ('EC-Euratom'). Neither the European Union nor the granting authority can be held responsible for them.

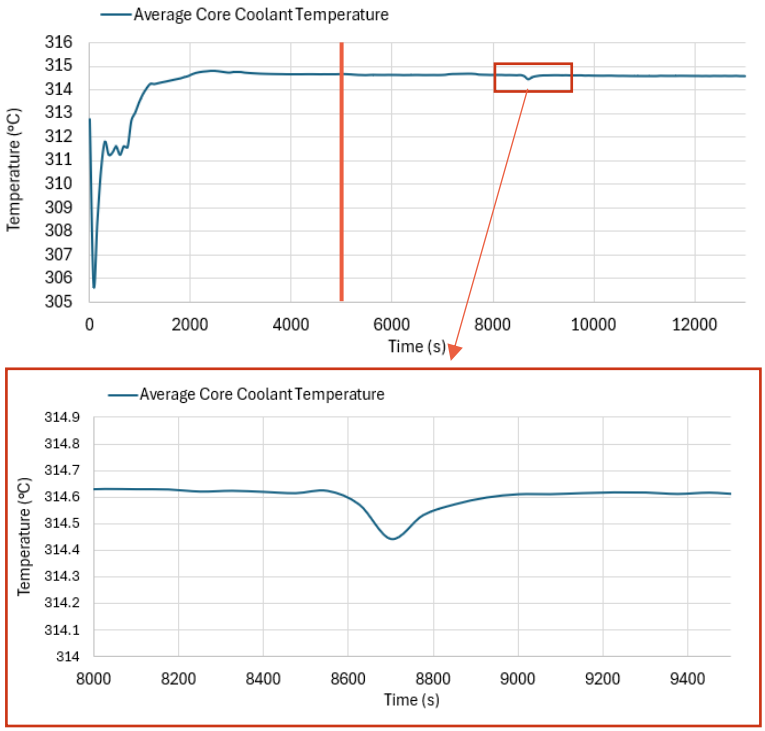

Figure 17: Average Core Coolant Temperature during thermal load rejection transient.

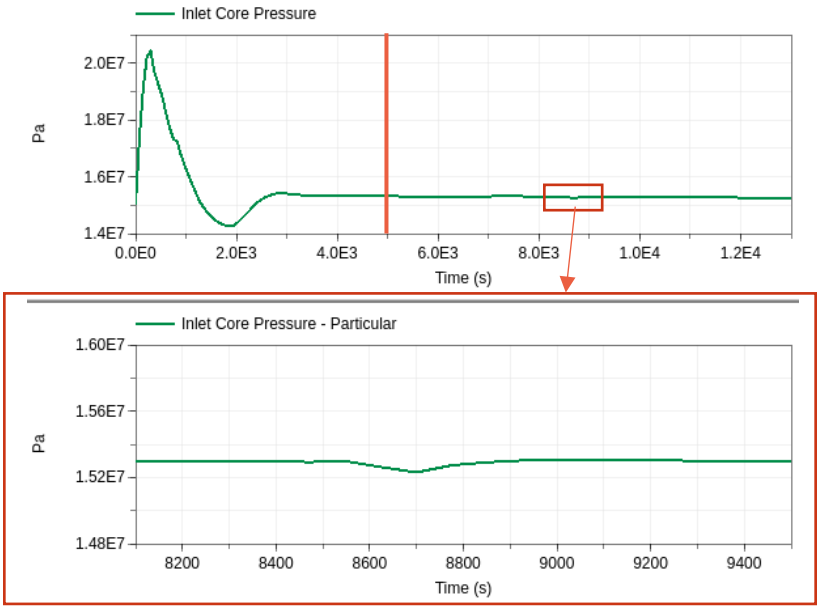

Figure 18: Inlet Core Pressure during thermal load rejection transient.

The opening of the cogeneration valve during the first increase of the thermal load led to the opening of the high-pressure turbine inlet valve and, at the same time, to the partial closure of the inlet valve to the medium-pressure turbine as shown in Figure 19. The two valves are controlled by the pressure at the inlet of the high-pressure and medium-pressure turbine respectively [5]. Again, after the occurrence of the thermal load rejection event, the two

Funded by the European Union

Funded by the European Union. Views and opinions expressed are however those of the author(s) only and do not necessarily reflect those of the European Union or the European Atomic Energy Community ('EC-Euratom'). Neither the European Union nor the granting authority can be held responsible for them.

components were brought to the full-electric power generation condition through a steep ramp. However, as shown in Figure 19, the medium-pressure turbine inlet valve opening experienced a mild peak before stabilizing on the full-electric value, probably due to the related control system response to the steep changes in the operating conditions. In this regard, it must be mentioned that the sharp response of the BOP components to the changes brought by the thermal load rejection event may be influenced by the fact that the BOP is quasi-static.

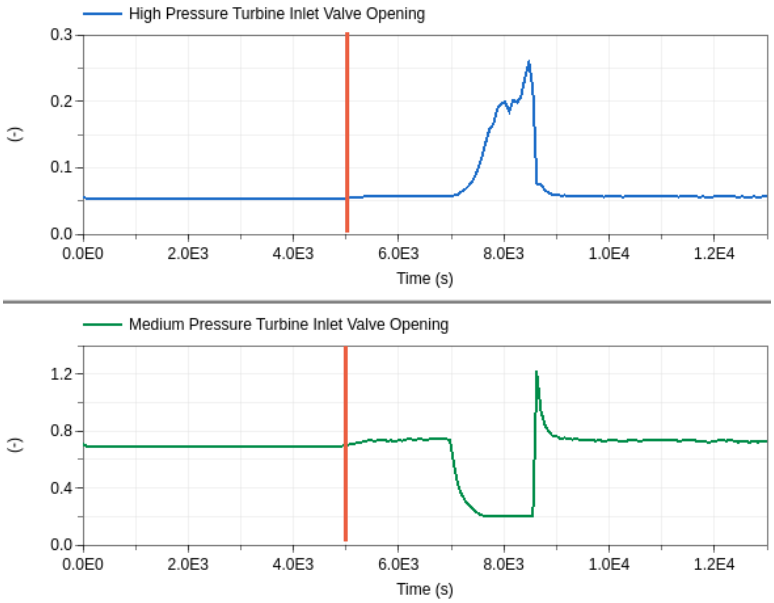

Figure 19: High pressure and medium pressure turbine inlet valves opening during thermal load rejection transient.

Following the thermal load rejection, the openings of the high- and medium-pressure turbine inlet valves led to the steam mass flow rate entering the turbines to suddenly decrease and increase, respectively, as shown in Figure 20 and Figure 21. However, it can be noticed how the action of the inlet turbine pressure control systems was found to be correctly working, the pressure at the inlet of both turbines being kept constant along the entire transient (see again Figure 20 and Figure 21).

Funded by the European Union

Funded by the European Union. Views and opinions expressed are however those of the author(s) only and do not necessarily reflect those of the European Union or the European Atomic Energy Community ('EC-Euratom'). Neither the European Union nor the granting authority can be held responsible for them.

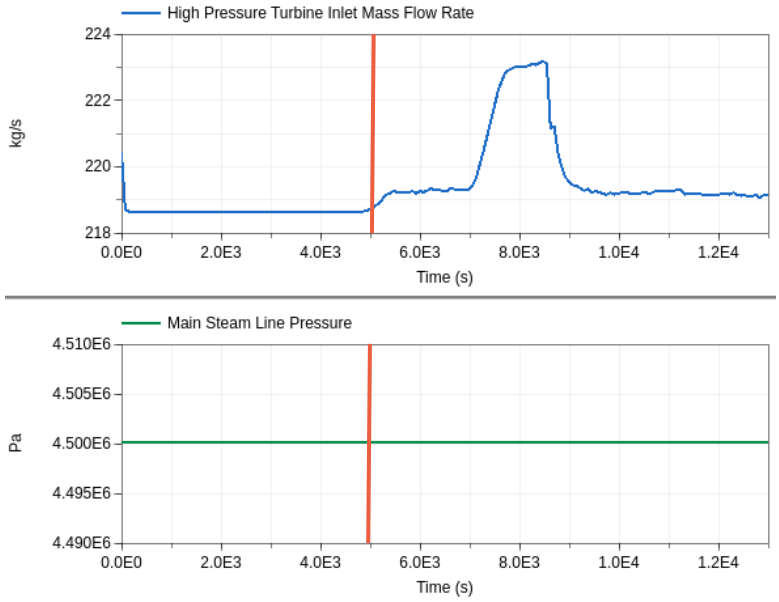

Figure 20: High pressure turbine inlet mass flow rate and main steam line pressure during thermal load rejection transient.

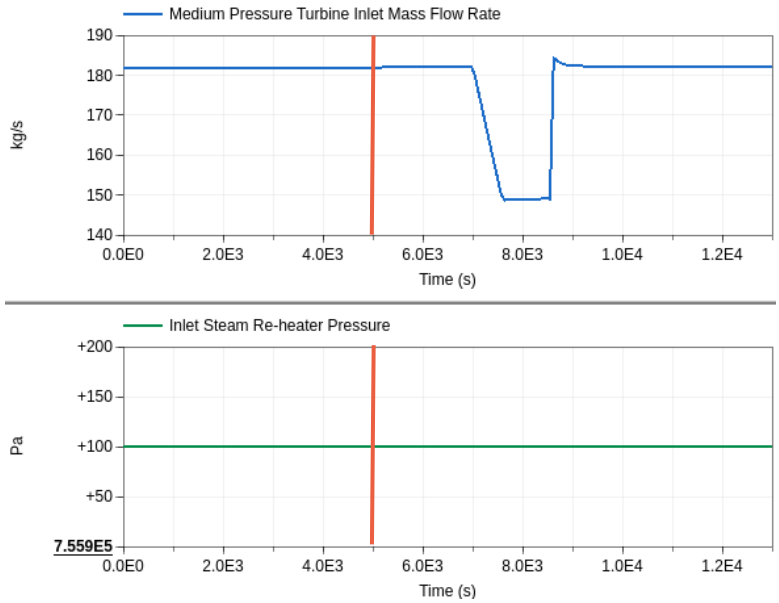

Figure 21: Medium pressure turbine inlet mass flow rate and measured pressure at steam re-heater inlet during thermal load rejection transient.

The obtained changes of the steam mass flow rate feeding the steam turbines led to the predictable decrease of the BOP electrical power during the cogeneration valve opening, whereas it was brought to the rated threshold after the thermal load rejection event as shown in Figure 22.

Funded by the European Union

Funded by the European Union. Views and opinions expressed are however those of the author(s) only and do not necessarily reflect those of the European Union or the European Atomic Energy Community ('EC-Euratom'). Neither the European Union nor the granting authority can be held responsible for them.

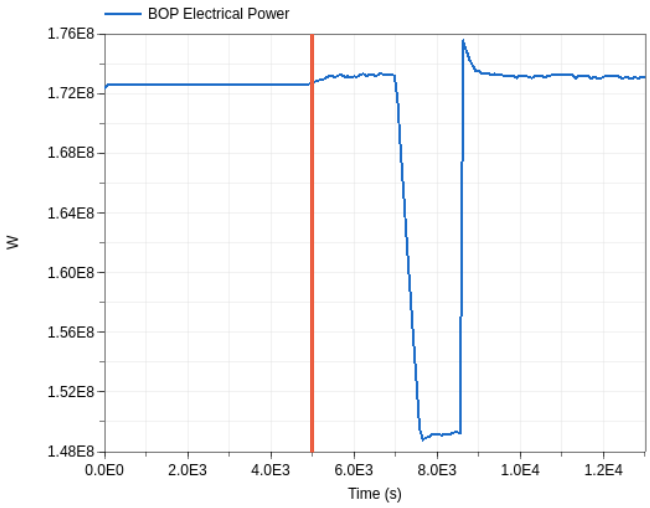

Figure 22: BOP electrical power during thermal load rejection transient.

To finalize this section, the following conclusions can be drawn:

- The coupling between CATHARE 3 and MODELICA, using Dymola 24x as co-simulation supervisor and quasi-static BOP model, was found to be robust enough in handling steep changes in the boundary conditions, thus restoring the coupled system behaviour to the full-electric case after the thermal load rejection transient occurrence.
- The predicted impact of the presently assessed AOOs on the primary circuit has resulted to be mild in terms of temperature and pressure excursion of the primary coolant and the core power rising, which went above the nominal value of about 0.8 % only.
- Basing on the adopted simplified BOP layout, therefore, the results predict that by transferring the rejected cogeneration heat load to the turbine, effects of a load change of about 15 % of thermal power could be controlled without triggering safety systems or changing primary side parameters significantly.

Moreover, even though the results were likely influenced by the neglected component dynamics, the steep changes of the mass flow rate entering the medium pressure turbine and of the electrical power may suggest further assessment about the capability of the steam turbines and of the electrical grid in dealing with such sudden excursions. In this regard, it can be reminded that the adoption of a different control strategy, together with a dynamic BOP, could dump the sudden variations of the parameter to keep them within specified thresholds dictated by the safety limits of all the involved system and grid components.

Funded by the European Union

Funded by the European Union. Views and opinions expressed are however those of the author(s) only and do not necessarily reflect those of the European Union or the European Atomic Energy Community ('EC-Euratom'). Neither the European Union nor the granting authority can be held responsible for them.

4. Conclusions and recommendations

Within TANDEM WP4 it was shown that the coupled code system consisting of MODELICA and the thermal-hydraulic system codes ATHLET or CATHARE is applicable to various AOOs. The investigated thermal load rejection transients show that the E-SMR and its control systems can compensate the loss of load on the secondary side. The reactivity feedbacks of the core and the moderator as well as the control of the core power by the control rods can keep the reactor in a safe operating condition reasonably well and not require a SCRAM. When secondary side steam/heat flows can be redistributed between power generation and cogeneration heat demands, load rejections of the cogeneration part only have a small impact on primary side parameters.

However, if secondary heat demand is suddenly increased at full power, which was exemplarily simulated by a cogeneration heat demand increase, the core power will exceed its nominal value. This might be acceptable depending on the actual design of the E-SMR. However, normally a limitation system would be part of the reactor design which would limit the core power in those cases. Such a limitation system was not part of the current study.

It can additionally be noticed that besides the time-demanding implementation of the coupling between the codes also the adjustments of the different parameters in the inputs were time-consuming. For instance, in ATHLET the different parameters for all PI-controllers needed to be set suitably to avoid program crashes on the MODELICA side due to unphysical properties or backflows. When the parameters were finally adjusted, however, the different simulations were possible and stable.

Funded by the European Union

Funded by the European Union. Views and opinions expressed are however those of the author(s) only and do not necessarily reflect those of the European Union or the European Atomic Energy Community ('EC-Euratom'). Neither the European Union nor the granting authority can be held responsible for them.

5. References

[1] E-SMR Dataset, ELSMOR Project, download from website: https://etsin.fairdata.fi/dataset/00b62da2-7b96-4e70-82ef-1e8afaa0ecb1, last visit: 29.08.2024

[2] Calogera Lombardo, Massimiliano Polidori, Marco Ricotti, Guido Masotti, Alessandro De Angelis, Andrea Pucciarelli, D2.6 – CATHARE SMR model description, Deliverable D2.6, TANDEM Project, 2024

[3] Sebastian Buchholz, Fabian Weyermann, D2.7 – ATHLET SMR model description, Deliverable D2.7 TANDEM Project, 2024

[4] IAEA, Guidance on Nuclear Cogeneration, IAEA Nuclear Energy Series No. NP-T-1.17, Vienna, 2019

[5] G. Simonini, Y. Hammadi, D2.3 – Modelica models description for the 'TANDEM' library, Deliverable D2.3, TANDEM Project, 2024

[6] Modelica Association, Modelica Standard Library Official GitHub Repository, https://github.com/modelica/ModelicaStandardLibrary, accessed on: February 12th, 2024.

[7] Brück, D., Elmqvist, H., Olsson, H. and Mattsson, S. E., (2002), Dymola for Multi-Engineering Modelling and Simulation, 2nd International Modelica Conference, Proceedings, pp. 55-1-55-8, March 18-19, Oberpfaffenhofen, Germany.

[8] Petzold, L. R., (1982), A description of DASSL: A differential/algebraic system solver, Conference Proceedings of 10th IMACS World Congress, August 8-13, Montreal, Canada, OSTI ID:5882821.

[9] International Atomic Energy Agency (IAEA): Deterministic Safety Analysis for Nuclear Power Plants, Specific Safety Guide. IAEA Safety Standards Series, SSG-2 (Rev. 1), ISBN 978-92-0-102119-9, IAEA, 2019.

[10] Schöffel, P. J., Di Nora, V. A., Eckert, D., Junk, M., Cron, D. von der, Weyermann, F., Wielenberg, A.: ATHLET 3.4.1 Models and Methods. Gesellschaft für Anlagen- und Reaktorsicherheit (GRS) gGmbH, GRS-P-1/Vol. 4 Rev. 9, May 2024.

Funded by the European Union

Funded by the European Union. Views and opinions expressed are however those of the author(s) only and do not necessarily reflect those of the European Union or the European Atomic Energy Community ('EC-Euratom'). Neither the European Union nor the granting authority can be held responsible for them.